



This discussion paper is/has been under review for the journal Biogeosciences (BG).  
Please refer to the corresponding final paper in BG if available.

# Mineral dust aerosol from Saharan desert by means of atmospheric, emission, dispersion modelling

**F. Guarnieri<sup>1,2</sup>, F. Calastrini<sup>1,2</sup>, C. Busillo<sup>1,2</sup>, M. Pasqui<sup>2</sup>, S. Becagli<sup>3</sup>, F. Lucarelli<sup>4</sup>,  
G. Calzolai<sup>4</sup>, S. Nava<sup>4</sup>, and R. Udisti<sup>3</sup>**

<sup>1</sup>LAMMA Consortium, Via Madonna del Piano 10, 50019 Sesto Fiorentino (FI), Italy

<sup>2</sup>IBIMET, National Research Council, Via G. Caproni 8, 50145 Firenze (FI), Italy

<sup>3</sup>Chemical Department, Florence University, Via della Lastruccia 3,  
50019 Sesto Fiorentino (FI), Italy

<sup>4</sup>Physics Department, Florence University and National Institute of Nuclear Physics (INFN) –  
Florence, Via G. Sansone 1, 50019 Sesto Fiorentino (FI), Italy

Received: 15 June 2011 – Accepted: 17 June 2011 – Published: 22 July 2011

Correspondence to: F. Guarnieri (f.guarnieri@ibimet.cnr.it)

Published by Copernicus Publications on behalf of the European Geosciences Union.

**BGD**

8, 7313–7338, 2011

Mineral dust aerosol  
from Saharan desert

F. Guarnieri et al.

[Title Page](#)

[Abstract](#)

[Introduction](#)

[Conclusions](#)

[References](#)

[Tables](#)

[Figures](#)

◀

▶

◀

▶

[Back](#)

[Close](#)

[Full Screen / Esc](#)

[Printer-friendly Version](#)

[Interactive Discussion](#)



## Abstract

The application of Numerical Prediction Models to mineral dust cycle is considered of prime importance for the investigation of aerosol and non-CO<sub>2</sub> greenhouse gases contributions in climate variability and change. In this framework, a modelling system 5 was developed in order to provide a regional characterization of Saharan dust intrusions over Mediterranean basin. The model chain is based on three different modules: the atmospheric model, the dust emission model and transport/deposition model. Numerical simulations for a selected case study, June 2006, were performed in order to evaluate the modelling system effectiveness. The comparison of the results obtained in 10 such a case study shows a good agreement with those coming from GOCART model. Moreover a good correspondence was found in the comparison with in-situ measurements regarding some specific crustal markers in the PM<sub>10</sub> fraction.

## 1 Introduction

Dust storm formation is closely related with local and large-scale climate variability 15 and related anomalies, deforestation, vegetation destruction, species extinction and greenhouse effect. In fact, the mineral dust aerosol injected into the atmosphere and transported away may modify the direct radiative forcing, the marine biochemistry, the air quality, with consequence on human health and visibility. Furthermore it can play a role in the neutralization of acid rain.

20 The numerical modelling system developed to study the processes of desert dust emission, transport and deposition is based on different modules, to take into account the natural phenomena involved in the dust cycle in the atmosphere. The dust cycle consists of two major physical mechanisms: first, a wind stress lifting mechanism able to raise up dust particles from some type of bare soil surfaces; second, a long range 25 transport mechanism with a high degree of spatial coherence. Moreover, a 3-D modelling system performs a good description of all the vertical layers, accounting for the infiltration of aerosol above the boundary layer.

[Title Page](#)

[Abstract](#)

[Introduction](#)

[Conclusions](#)

[References](#)

[Tables](#)

[Figures](#)

[◀](#)

[▶](#)

[◀](#)

[▶](#)

[Back](#)

[Close](#)

[Full Screen / Esc](#)

[Printer-friendly Version](#)

[Interactive Discussion](#)



A case study, regarding a Saharan dust intrusion on Mediterranean Basin during June 2006, is here presented. In order to test for the modelling system capability, the results are compared with those obtained by the application of the global model GO-CART ([http://disc.sci.gsfc.nasa.gov/gesNews/gocart\\_data\\_V006](http://disc.sci.gsfc.nasa.gov/gesNews/gocart_data_V006)) and with some available in-situ measurements.

As a further development, it is possible to run the model chain for a more extended period to create a complete climatology for this kind of events, in the framework of climate change.

## 2 Methodology

10 A 3-D comprehensive atmospheric emission and dispersion numerical modelling system is developed for the computational domain showed in Fig. 1, in order to provide a regional characterization of Saharan dust intrusion over Mediterranean basin.

15 The Numerical Prediction Models is based on three different modules: the atmospheric model, the dust emission model and the transport/deposition model, acting following the scheme of Fig. 2.

16 The Regional Atmospheric Modelling System (RAMS) (Pielke et al., 1992), forced by the Reanalysis2 atmospheric dataset, provides the input data for the other modules. The dust emission model, called DUSTEM, simulates the emission of four particle categories, based on the content of clay, small-silt, large-silt and sand from the Saharan desert. The third module, the Comprehensive Air quality Model with extensions (CAMx) (<http://www.camx.com/>), forced by the RAMS meteorological fields and by the emission amount from DUSTEM, provides the dynamical transport and deposition of the dust particles.

BGD

8, 7313–7338, 2011

Mineral dust aerosol  
from Saharan desert

F. Guarnieri et al.

[Title Page](#)

[Abstract](#)

[Introduction](#)

[Conclusions](#)

[References](#)

[Tables](#)

[Figures](#)

◀

▶

◀

▶

[Back](#)

[Close](#)

[Full Screen / Esc](#)

[Printer-friendly Version](#)

[Interactive Discussion](#)



## 2.1 The Regional Atmospheric Modelling System (RAMS)

The Regional Atmospheric Modelling System (RAMS) is constructed around the full set of non-hydrostatic, compressible equations that describe the atmospheric dynamics and thermodynamics.

5 The used RAMS version is the 6.02, performed on parallel computing, on the computational domain shown in Fig. 2, containing a big part of the Northern Hemisphere, in order to catch all the dynamic mechanism involved in the description of this events. To perform and compute the RAMS simulations, the initial and boundary atmospheric conditions need to be set. Further, the regional model needs to be forced during the period  
10 of simulation by providing observed or reconstructed datasets to the model. To address these necessities, the Reanalysis2 dataset (Kanamitsu et al., 2002) was employed, with a 2.5 degree of horizontal resolution; specifically the geopotential height, temperature, relative humidity, zonal wind component, meridional wind component fields are employed and forced, as boundary conditions, every 6 h throughout the simulation  
15 period.

The performed simulation period is from 1 to 30 June 2006. The configuration is set with the following features:

- 200 × 80 grid points, 32 vertical levels, 11 soil levels;
- horizontal resolution: 60 km;
- vertical resolution: variable on sigma levels with a stretching factor, in order to obtain a greater resolution near to the soil and a smaller one above 2000 m;
- output temporal resolution: 1 h;
- time-step: 120 s;
- activated parameterization schemes: convective scheme by Kain-Fritsch.

[Title Page](#)

[Abstract](#)

[Introduction](#)

[Conclusions](#)

[References](#)

[Tables](#)

[Figures](#)

[◀](#)

[▶](#)

[◀](#)

[▶](#)

[Back](#)

[Close](#)

[Full Screen / Esc](#)

[Printer-friendly Version](#)

[Interactive Discussion](#)



## 2.2 The dust emission model DUSTEM

Wind erosion of soil is the physical movement of soil particles by wind energy. The main factors determining inherent risk of wind erosion are soil type, vegetation cover, soil moisture content, and surface atmospheric turbulence (Tegen and Fung, 1994;

5 Fecan et al., 1999; Gillette, 1980; Gong et al., 2003; Marticorena and Bergametti, 1995; Qian et al., 2001).

In order to estimate dust emissions, a standalone model called DUST Emission Model (DUSTEM) was developed. DUSTEM is based on the DREAM model, developed by Insular Coastal Dynamics, MALTA (ICoD) (Nickovic et al., 2001). The model 10 estimates the dust emission rates using empirical relationships based on soil texture and friction velocity. In fact, the released surface concentration of mobilized particles and the corresponding surface vertical fluxes depend on both the soil structure and the turbulent state of the surface atmosphere.

Different soil types act as different dust sources depending on their particle size, 15 density, and dust productivity. Further, the effective surface vertical flux depends on soil moisture, because it reduces the amount of dust injected into atmosphere.

The adopted emission model seems to reproduce the phenomenon of dust emission in a good way, since it takes into account the most important factor and allows the differentiation of the emissions for different soil types. The model computes emission 20 rates for four dimensional classes: clay, silt small, silt large, sand (Nickovic et al., 2001; Tegen and Fung, 1994). The main physical features of these classes are shown in Table 1.

For the selected case study involving June 2006, the run of the DUSTEM model provides the emission rates with a temporal resolution of 1 h. The horizontal resolution 25 of the DUSTEM outputs must be the same as the CAMx model one, which is 30 km. For this reason, the meteorological RAMS input data for DUSTEM model were been downscaled from a resolution of 60 to 30 km. The maps of emission rates cumulated on the whole period of the simulation, relative to the first and the second dimensional classes, are shown in Fig. 3.

[Title Page](#)

[Abstract](#)

[Introduction](#)

[Conclusions](#)

[References](#)

[Tables](#)

[Figures](#)

[◀](#)

[▶](#)

[◀](#)

[▶](#)

[Back](#)

[Close](#)

[Full Screen / Esc](#)

[Printer-friendly Version](#)

[Interactive Discussion](#)



## 2.3 The transport/deposition model CAMX

The Comprehensive Air quality Model with extensions is an Eulerian photochemical dispersion model that allows for an integrated “one-atmosphere” assessment of gaseous and particulate air pollution over many scales ranging from urban to super-regional.

CAMx simulates the transport, chemical reactions, and removal of pollutants in the troposphere by solving the pollutant continuity equation for each species.

As far as the aerosol deposition is concerned, the algorithm of Slinn and Slinn (1980) was used for the dry deposition, while for the wet one the algorithm was by Seinfeld and Pandis (1998).

To simulate the transport and deposition of mineral dust, the chemical module was been switched off. CAMx model run on a computational domain slightly smaller of RAMS's one, with an extension of  $11\,400 \times 10\,200 \text{ km}^2$ . The computational domain in Polar Stereographic coordinate (with pole in  $40^\circ \text{ N}$  and  $5^\circ \text{ E}$ ), is formed by  $380 \times 340$  cells with  $30 \text{ km}$  of resolution. There are 18 vertical levels, from 10 to  $10\,500 \text{ m}$ , with a better resolution near the ground. The meteorological input files for CAMx were interpolated from 60 to  $30 \text{ km}$  of resolution. The input files containing the emission rates for the four dimensional soil classes, coming from DUSTEM, are described in Sect. 2.2.

Particularly, a run was performed for each single dimensional class. The initial and boundary conditions are set to zero. Only the results of the first two soil classes are discussed, because they are the ones involved in long-range transport.

BGD

8, 7313–7338, 2011

Mineral dust aerosol  
from Saharan desert

F. Guarnieri et al.

[Title Page](#)

[Abstract](#)

[Introduction](#)

[Conclusions](#)

[References](#)

[Tables](#)

[Figures](#)

◀

▶

◀

▶

[Back](#)

[Close](#)

[Full Screen / Esc](#)

[Printer-friendly Version](#)

[Interactive Discussion](#)



### 3 Meteorological analysis

#### 3.1 Physical mechanisms for dust emission, transport and deposition

The propitious atmospheric synoptic and soil conditions for raising up the mineral dust into the atmosphere are well known, as the necessary conditions for the transport into the Mediterranean basin (Yair et al., 2001). The dust emission always comes with an advection of air masses coming from North Europe or Balkans regions to Algeria, Libya and Egypt up to Chad. These air masses are characterized by strong and constant wind in the lower layers of the atmosphere, with thermal gradient. These deep intrusions are relatively rare during the Spring-Summer months, about 6 per year (Vizy and Cook, 2009). Despite that, they are able to move a big quantity of dust, which can remain up in the atmosphere, above the boundary layer, waiting for other physical mechanisms that take them far from emission area (Washington et al., 2005).

The thermal gradient at ground level has two important effects in causing emission mechanism. The first one is due to the acceleration of the thermal wind on the surface, in the correspondence of the air mass front. In this way, it increases the soil friction, and consequently the energy necessary to rise up the dust. The orography could amplify these meteorological conditions. Secondly, the positive surface thermal gradient can reduce the moisture content of the soil, favouring the dust rising up mechanism.

Once the dust has been raised up above the boundary layer, it is necessary a deep and compact circulation between 850 and 700 hPa, which can transport the dust far from the emission area. There are two prevalent directions: the first one is due to the tropical African Easterly Waves, which moves the dust through the Atlantic Ocean; the second one goes directly on the Mediterranean basin and Europe. The latter needs a stationary cyclonic circulation on Iberian Peninsula and/or on France. In this case, with an anticyclonic circulation on North Africa (Morocco and Algeria), transports of dust for some thousand of kilometres in a short time are possible. There is the formation of dust jet, called “dust-plumes”.

[Title Page](#)[Abstract](#)[Introduction](#)[Conclusions](#)[References](#)[Tables](#)[Figures](#)[◀](#)[▶](#)[◀](#)[▶](#)[Back](#)[Close](#)[Full Screen / Esc](#)[Printer-friendly Version](#)[Interactive Discussion](#)

The dust deposition depends on dry removal mechanism, as the gravity effect, or on wet removal caused by some precipitation events.

### 3.2 Synoptic description of June 2006

The studied event has a temporal extension of about 20 days, as far as the atmospheric mechanism is concerned. The Hovmöller latitude/time diagram for the temperature anomaly at 850 hPa, obtained as the mean value on the longitudinal band from 15° E to 40° E is represented in Fig. 4. The temperature anomaly is evaluated between each day of the investigated period and the mean value for June 2006. From 4 June a big descent of air mass, coming from North Europe to 25° N, lasts until 15 June, even if its thermo-dynamical conditions change. As shown in Fig. 4, there is an air descent also in the band 10° W–10° E, relatively cooler, during the first days of June.

During the same period, as it is shown by the zonal and meridional wind components of Fig. 5, there is a strong and persistent wind flux, which is one of the responsible mechanism for the dust emission in both the analysed longitudinal bands.

Analysing the wind field, the westerly propagation at 20° N–35° N is persistent during the period 4–17 June in the eastern sector, while the meridional propagation is much longer, even if the deep phase ends around 21 June. At the northern latitudes on the Mediterranean basin the direction changes after 15 June.

In fact, from 15 to 20 June the prevalent circulation is from South-West/West, giving the favourable condition for the dust transport over Europe.

In Fig. 6, the Geopotential Heights at 850 hPa are shown, respectively on 10° W–10° E and 15° E–40° E are shown, for the June month. The driving mechanism for the surface fluxes, which last for some days, is the high pressure on Morocco and Algeria, probably generated by the Heat Low System.

This phenomenon is usually indicated as an integral part of the West Africa monsoon system that develops starting from June. Its persistence and its intensity change a lot during the time, and they depend not only from the air heating, but also from the Atlantic fluxes.

[Title Page](#)[Abstract](#)[Introduction](#)[Conclusions](#)[References](#)[Tables](#)[Figures](#)[◀](#)[▶](#)[◀](#)[▶](#)[Back](#)[Close](#)[Full Screen / Esc](#)[Printer-friendly Version](#)[Interactive Discussion](#)

## 4 Results and discussion

### 4.1 Analysis of the mineral dust event – June 2006

Analysing the simulations results, from 6 June the desert dust arrives up to the Iberian Peninsula, as a consequence of the anticyclonic circulation over Morocco. In the following days the dust reaches North Europe (France, UK, Norway); from 16 June it reaches also the northern part of Italy. During 17 and 18 Spain, France, Swiss, Germany, Italy and Balcanic Peninsula are interested by strong dust concentrations (Fig. 7).

In the last days of June a big area from West Mediterranean basin to Scandinavian Peninsula and Russia is interested by mineral dust both at lower and upper levels. In 10 24 and 25 June the Italian peninsula is affected by a decrease of dust concentration in the lower vertical levels, because of the irruption of a cyclonic mass coming from the Atlantic region, which momentarily interrupts the south-western flux on Italy. After those days the transport mechanism restarts again until the end of June.

During the whole simulation period the model results show a Saharan dust flux moving through Atlantic Ocean due to the tropical African Easterly Waves.

Focusing on Mediterranean basin, until 25 June, the concentration at the soil of the particle range 1–2 µm (CCR1, Table 1) is higher than the second class (CCR2, Table 1), while in the last period, from 26 to the end of June, both concentrations are quite similar. The vertical sections of the mean daily dust concentration for the first two fractions, at 20 the latitude 43.78° N, corresponding to the European Regions of Mediterranean area, are shown in Fig. 8. The dust is incoming on France and Spain, both at low and high levels until 5000–7000 m. The greatest dust concentration values over Europe are reached during the period 16–22 June: the higher values are achieved between 1000 and 8000 m, while under the boundary layer the concentrations are lower, about one order of magnitude ( $30\text{--}40\text{ }\mu\text{g m}^{-3}$  vs.  $200\text{--}500\text{ }\mu\text{g m}^{-3}$ ). The longitudinal sections too show the Saharan dust transport over European regions, as displayed in Fig. 9.

[Title Page](#)[Abstract](#)[Introduction](#)[Conclusions](#)[References](#)[Tables](#)[Figures](#)[◀](#)[▶](#)[◀](#)[▶](#)[Back](#)[Close](#)[Full Screen / Esc](#)[Printer-friendly Version](#)[Interactive Discussion](#)

## 4.2 Model evaluation

To test the models chain performances, the results were compared with the maps provided by GOCART global model as well as with in-situ PM<sub>10</sub> composition measurements.

### 5 4.2.1 Comparison with GOCART model

A first comparison was made using GOCART model, which is a global model developed by the Georgia Institute of Technology-Goddard to simulate the aerosol optical thickness for dust, organic and black carbon, sulphate and sea salt (Chin et al., 2002). GOCART dust aerosol optical depth daily maps were used ([http://disc.sci.gsfc.nasa.gov/gesNews/gocart\\_data\\_V006](http://disc.sci.gsfc.nasa.gov/gesNews/gocart_data_V006)).

10 The approach used by GOCART model to estimate the dust aerosol contribution is consistent with the method used by RAMS-DUSTEM-CAMx model system, but the images provided by NASA are given as optical thickness and not as dust concentration. The dust aerosol column optical depths (550 nm) from GOCART are represented in  
15 Fig. 10 for 16 and 20 June 2006. Comparing Fig. 10 with Fig. 7, there is a very good agreement between the CAMx and GOCART simulated events, for both temporal and spatial distributions.

### 4.2.2 Comparison model/measurements

20 For the selected case study, some specific in situ measurements were available in the framework of PATOS Project, which was funded by the Tuscany Regional Government to investigate the aerosol composition and to identify its sources (<http://servizi.regione.toscana.it/aria/index.php?idDocumento=18348>). One of the Project aims was to evaluate the natural contribution to the total amount of PM<sub>10</sub>, with particular attention to  
25 the Saharan dust intrusions. To this end, some specific analysis techniques, like PIXE (*Particle Induced X-ray Emission*) (Johansson and Campbell, 1978), have been used

[Title Page](#)

[Abstract](#)

[Introduction](#)

[Conclusions](#)

[References](#)

[Tables](#)

[Figures](#)

[◀](#)

[▶](#)

[◀](#)

[▶](#)

[Back](#)

[Close](#)

[Full Screen / Esc](#)

[Printer-friendly Version](#)

[Interactive Discussion](#)



Mineral dust aerosol  
from Saharan desert

F. Guarnieri et al.

[Title Page](#)[Abstract](#)[Introduction](#)[Conclusions](#)[References](#)[Tables](#)[Figures](#)[◀](#)[▶](#)[◀](#)[▶](#)[Back](#)[Close](#)[Full Screen / Esc](#)[Printer-friendly Version](#)[Interactive Discussion](#)

To improve the performance of the models chain in the lower levels of the atmosphere, it could be useful to introduce a nested grid, with a higher resolution, over the target area, where the measurements site are located.

## 5 Conclusions

5 The aim of this study was the evaluation of the strength of numerical modelling system in the reconstruction of mineral dust cycle. A comprehensive atmospheric, emission, dispersion modelling system was developed in order to provide a regional characterization of Saharan dust intrusions over Mediterranean basin. For the selected case study, June 2006, the model results were compared with maps provided by GOCART, 10 showing a good agreement for both temporal and spatial distributions. Further, the modelling system results were compared with in-situ measurements of some specific crustal markers in the  $PM_{10}$  fraction, showing a good agreement. Nevertheless, the model gives lower values than the measurements in a specific case (sampling station in a seaside). Probably, the reason could be traced to the model representation of 15 the boundary layer vertical extent, which could be underestimated near to the coast. It could be useful to introduce a nested grid, with a higher resolution, over the target area, where the measurement sites are located. However, also the calculation of the Saharan contribution by the use of measured data may be further improved by the subtraction of the local soil dust contribution.

20 It is also possible to run the model for a more extended period and to create a complete climatology for these kinds of events, in the framework of climate change.

25 *Acknowledgements.* The authors would like to acknowledge the Tuscany Regional Government (Italy), which supported the PATOS project and provided the experimental data here used. The authors would like to acknowledge also Giovanni online data system, developed and maintained by the NASA GES DISC for the dust maps, used in this study.

[Title Page](#)[Abstract](#)[Introduction](#)[Conclusions](#)[References](#)[Tables](#)[Figures](#)[◀](#)[▶](#)[◀](#)[▶](#)[Back](#)[Close](#)[Full Screen / Esc](#)[Printer-friendly Version](#)[Interactive Discussion](#)

## References

Borbely-Kiss, I., Kiss, A. Z., Koltay, E., Szabo, G., and Bozo, L.: Saharan dust episodes in Hungarian aerosol: Elemental signatures and transport trajectories. *J. Aerosol Sci.*, 35, 1205–1224, 2004.

5 Chiari, M., Lucarelli, F., Mazzei, F., Nava, S., Paperetti, L., Prati, P., Valli, G., and Vecchi, R.: Characterization of airborne particulate matter in an industrial district near Florence by PIXE and PESA, *X-Ray Spectrom.*, 34, 323–329, doi:10.1002/xrs.825, 2005.

10 Chin, M., Ginoux, P., Kinne, S., Torres, O., Holben, B. N., Duncan, B. N., Martin, R. V., Logan, J. A., and Higurashi, A.: Tropospheric aerosol optical thickness from the GOCART model and comparisons with satellite and sunphotometer measurements, *J. Atmos. Sci.*, 59, 461–483, 2002.

ENVIRON Web site: <http://www.camx.com/>, access: 5 July 2011.

15 Fécan, F., Marticorena, B., and Bergametti, G.: Parametrization of the increase of the aeolian erosion threshold wind friction velocity due to soil moisture for arid and semi-arid areas, *Ann. Geophys.*, 17, 149–157, doi:10.1007/s00585-999-0149-7, 1999.

Gillette, D. A.: "Major Contributions of Natural Primary Continental Aerosols: Source Mechanisms", *Ann. NY Acad. Sci.*, 338, 348–358, 1980.

20 GOCART dataset: [http://disc.sci.gsfc.nasa.gov/gesNews/gocart\\_data\\_V006](http://disc.sci.gsfc.nasa.gov/gesNews/gocart_data_V006), access: 5 July 2011.

Gong, S. L., Zhang, X. Y., Zhao, T. L., Mckendry, I. G., Jaffe, D. A., and Lu, N. M.: Characterization of soil dust aerosol in China and its transport/distribution during 2001 ACE-Asia, 2. Model Simulation and Validation, *J. Geophys. Res.*, 108, 4262, doi:10.1029/2002JD002633, 2003.

25 Johansson, S. A. E and Campbell, J. L.: *PIXE A Novel Technique for Elemental Analysis*, John Wiley and Sons Ltd, 1978.

Kanamitsu, M., Ebisuzaki, W., Woollen, J., Yang, S. K., Hnilo, J. J., Fiorino, M., and Potter, G. L.: NCEP-DOE AMIP-II Reanalysis (R-2), *B. Am. Meteorol. Soc.*, 83, 1631–1643, 2002.

Marticorena, B. and Bergametti, G.: Modeling the atmospheric dust cycle: 1. Design of a soil derived dust emission scheme, *J. Geophys. Res.*, 100(D8), 16415–16430, 1995.

30 Mason, B.: *Principles of Geochemistry*, Wiley, New York, 1996.

Miranda, J., Cahill, T. A., and Morales, J. R.: Determination of Elemental Concentrations in Atmospheric Aerosols in Mexico City Using Proton Induced X-Ray Emission, *Proton Elastic*

BGD

8, 7313–7338, 2011

Mineral dust aerosol  
from Saharan desert

F. Guarnieri et al.

[Title Page](#)

[Abstract](#)

[Introduction](#)

[Conclusions](#)

[References](#)

[Tables](#)

[Figures](#)

◀

▶

◀

▶

[Back](#)

[Close](#)

[Full Screen / Esc](#)

[Printer-friendly Version](#)

[Interactive Discussion](#)



Nickovic, S., Kallos, G., Papadopoulos, A., and Kakaliagou, O.: A model for prediction of desert dust cycle in the atmosphere, *J. Geophys. Res.*, 106, 18113–18129, 2001.

Pielke, R. A., Cotton, W. R., Walko, R. L., Tremback, C. J., Lyons, W. A., Grasso, L. D., Nicholls, M. E., Moran, M. D., Wesley, D. A., Lee, T. J., and Copeland, J. H.: A comprehensive meteorological modeling system-RAMS, *Meteorol. Atmos. Phys.*, 49, 69–91, 1992.

Qian, W., Quan, L., and Shi, S.: Variations of the Dust Storm in China and its Climatic Control, *J. Climate*, 15, 1216–1228, 2001.

Seinfeld, J. H. and Pandis, S. N.: *Atmospheric chemistry and physics. From air pollution to climate change*, John Wiley and Sons, inc., New York, 1998.

Slinn, S. A. and Slinn, W. G. N.: Prediction for particle deposition on natural waters, *Atmos. Environ.*, 14, 1013–1016, 1980.

Tegen, I. and Fung, I.: Modeling of mineral dust in the atmosphere: Sources, transport, and optical thickness, *J. Geophys. Res.*, 99(D11), 22897–22914, 1994.

Vizy, E. K. and Cook, K. H.: A mechanism for African monsoon breaks: Mediterranean cold air surges, *J. Geophys. Res.*, 114, D01104, doi:10.1029/2008JD010654, 2009.

Washington, R., Todd, M. C., Engelstaedter, S., Mbainayel, S., and Mitchell, F.: Dust and the Low Level Circulation over the Bodélé Depression, Chad: Observations from BoDEx 2005, *J. Geophys. Res. Atmos.*, 111(D3), D03201, doi:10.1029/2005JD006502, 2006.

Yair, Y., Price, C., Levin, Z., Joseph, J., Israelevitch, P., Devir, P., Moalem, M., Ziv, B., and Asfur, M.: Sprite observations from the space shuttle during the Mediterranean Israeli Dust Experiment (MEIDEX), available at: <http://luna.tau.ac.il/~peter/MEIDEX/Publications/Paper2/Yoav1.htm>, 2001.

Title Page

Abstract

Introduction

Conclusions

References

Tables

Figures

◀

▶

◀

▶

Back

Close

Full Screen / Esc

Printer-friendly Version

Interactive Discussion



**Table 1.** Features of the four Typical Dust Particles.

Type	Name	Typical Particle Diameter ( $\mu\text{m}$ )	Typical Particle Radius ( $\mu\text{m}$ )	Particle Density ( $\text{g cm}^{-3}$ )	Erodible Fraction
Clay	CCR1	01–02	0.73	2.5	0.08
Silt, small	CCR2	02–20	6.1	2.65	1
Silt, large	CCR3	20–50	18	2.65	1
Sand	CCR4	50–100	38	2.65	0.12

[Title Page](#)[Abstract](#)[Introduction](#)[Conclusions](#)[References](#)[Tables](#)[Figures](#)[◀](#)[▶](#)[◀](#)[▶](#)[Back](#)[Close](#)[Full Screen / Esc](#)[Printer-friendly Version](#)[Interactive Discussion](#)

Mineral dust aerosol  
from Saharan desert

F. Guarnieri et al.

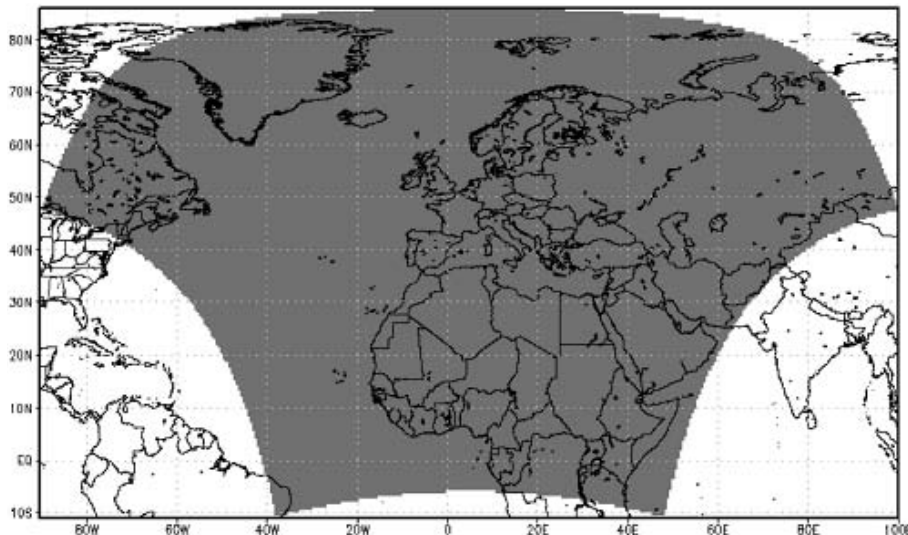


**Fig. 1.** Computational domain used for the RAMS simulations.

[Title Page](#)[Abstract](#)[Introduction](#)[Conclusions](#)[References](#)[Tables](#)[Figures](#)[◀](#)[▶](#)[◀](#)[▶](#)[Back](#)[Close](#)[Full Screen / Esc](#)[Printer-friendly Version](#)[Interactive Discussion](#)

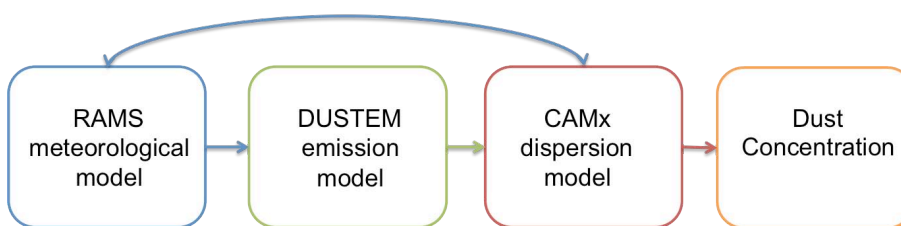


**Fig. 2.** Scheme of the model-chain RAMS-DUSTEM-CAMx.

[Title Page](#)[Abstract](#)[Introduction](#)[Conclusions](#)[References](#)[Tables](#)[Figures](#)[◀](#)[▶](#)[◀](#)[▶](#)[Back](#)[Close](#)[Full Screen / Esc](#)[Printer-friendly Version](#)[Interactive Discussion](#)

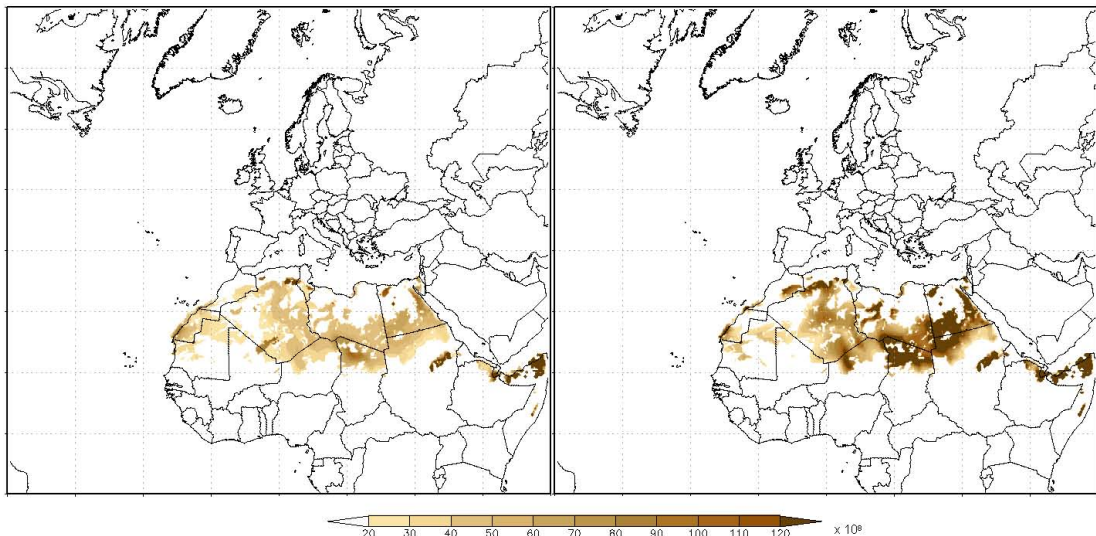


**Fig. 3.** Emission Rate, cumulated on the period 1–30 June 2006 for the first dimensional class (left) and for the second dimensional class (right) (values expressed in  $10^6 \text{ g h}^{-1}$ ).

[Title Page](#) | [Discussion Paper](#) | [Discussion Paper](#) | [Discussion Paper](#) | [Discussion Paper](#)

[Abstract](#) | [Introduction](#)  
[Conclusions](#) | [References](#)  
[Tables](#) | [Figures](#)

[◀](#) | [▶](#)  
[◀](#) | [▶](#)  
[Back](#) | [Close](#)

[Full Screen / Esc](#)

[Printer-friendly Version](#)  
[Interactive Discussion](#)

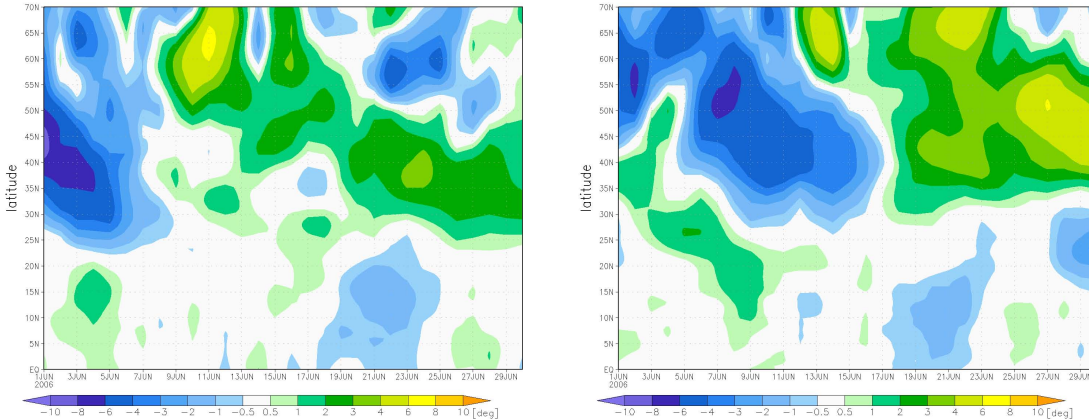


**Fig. 4.** Hovmöller latitude/time diagram for the temperature anomaly at 850 hPa, obtained as the mean on the longitudinal band from  $15^{\circ}$  E to  $40^{\circ}$  E (left) and on the longitudinal band from  $10^{\circ}$  W to  $10^{\circ}$  E (right).

[Title Page](#)[Abstract](#)[Introduction](#)[Conclusions](#)[References](#)[Tables](#)[Figures](#)[◀](#)[▶](#)[◀](#)[▶](#)[Back](#)[Close](#)[Full Screen / Esc](#)[Printer-friendly Version](#)[Interactive Discussion](#)

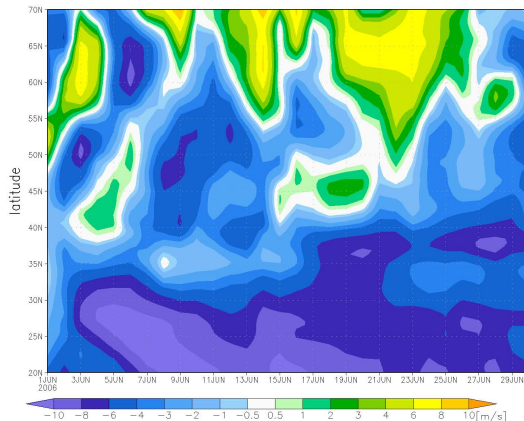
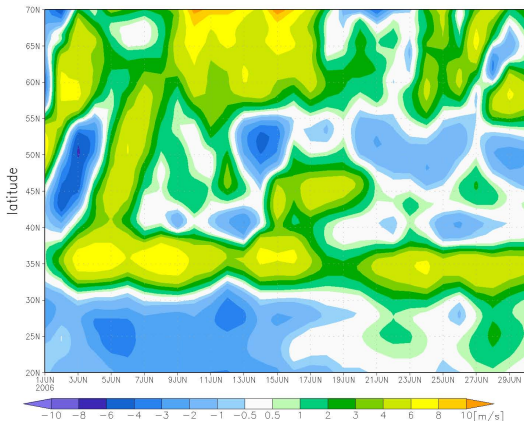


**Fig. 5.** Hovmöller latitude/time diagram for the zonal wind (left) and meridional wind (right) components at 850 hPa in the longitude band 15° E–40° E.

[Title Page](#)[Abstract](#)[Introduction](#)[Conclusions](#)[References](#)[Tables](#)[Figures](#)[◀](#)[▶](#)[◀](#)[▶](#)[Back](#)[Close](#)[Full Screen / Esc](#)[Printer-friendly Version](#)[Interactive Discussion](#)

Mineral dust aerosol  
from Saharan desert

F. Guarnieri et al.

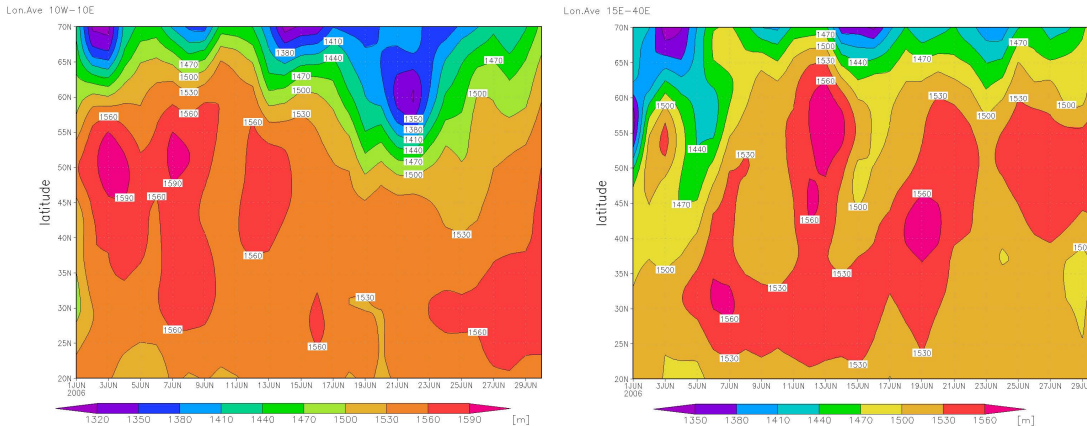


**Fig. 6.** Hovmöller latitude/time diagram for the Geopotential Height at 850 hPa in the longitude band  $10^{\circ}$  W– $10^{\circ}$  E (left) and  $15^{\circ}$  E– $40^{\circ}$  E (right).

[Title Page](#)[Abstract](#)[Introduction](#)[Conclusions](#)[References](#)[Tables](#)[Figures](#)[◀](#)[▶](#)[◀](#)[▶](#)[Back](#)[Close](#)[Full Screen / Esc](#)[Printer-friendly Version](#)[Interactive Discussion](#)

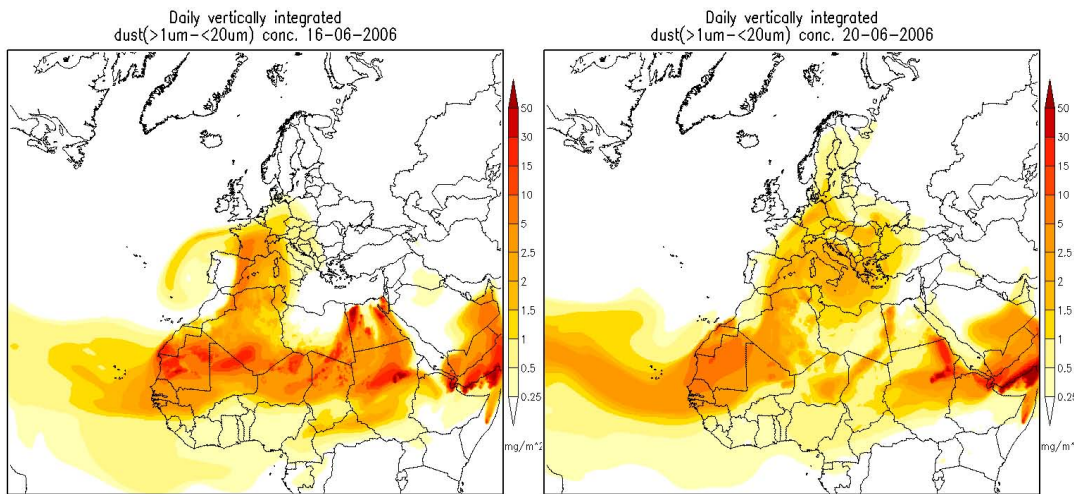


**Fig. 7.** Daily vertically integrated dust on 16 (left) and 20 (right) June, particle size 1–20  $\mu\text{m}$ .

- [Title Page](#)
- [Abstract](#) [Introduction](#)
- [Conclusions](#) [References](#)
- [Tables](#) [Figures](#)
- [◀](#) [▶](#)
- [◀](#) [▶](#)
- [Back](#) [Close](#)
- [Full Screen / Esc](#)

Printer-friendly Version

Interactive Discussion



Mineral dust aerosol  
from Saharan desert

F. Guarnieri et al.

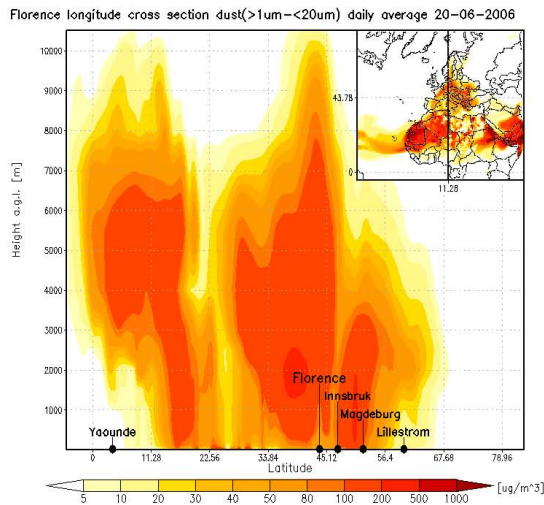
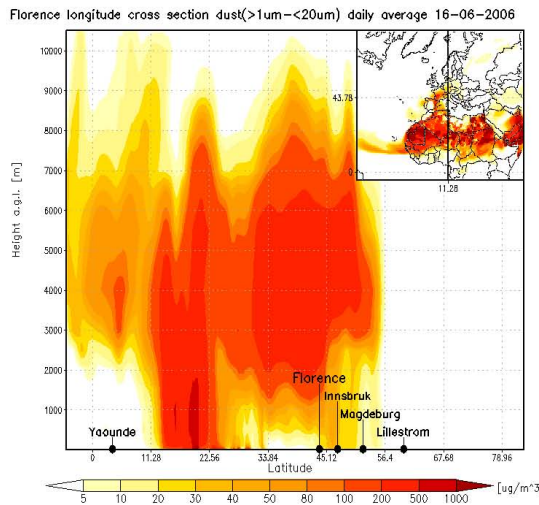


**Fig. 8.** Cross section at 43.78°N of the daily average of dust concentration, on 16 (left) and 20 June (right), particle size 1–20  $\mu\text{m}$ .

[Title Page](#)[Abstract](#)[Introduction](#)[Conclusions](#)[References](#)[Tables](#)[Figures](#)[◀](#)[▶](#)[◀](#)[▶](#)[Back](#)[Close](#)[Full Screen / Esc](#)[Printer-friendly Version](#)[Interactive Discussion](#)

Mineral dust aerosol  
from Saharan desert

F. Guarnieri et al.

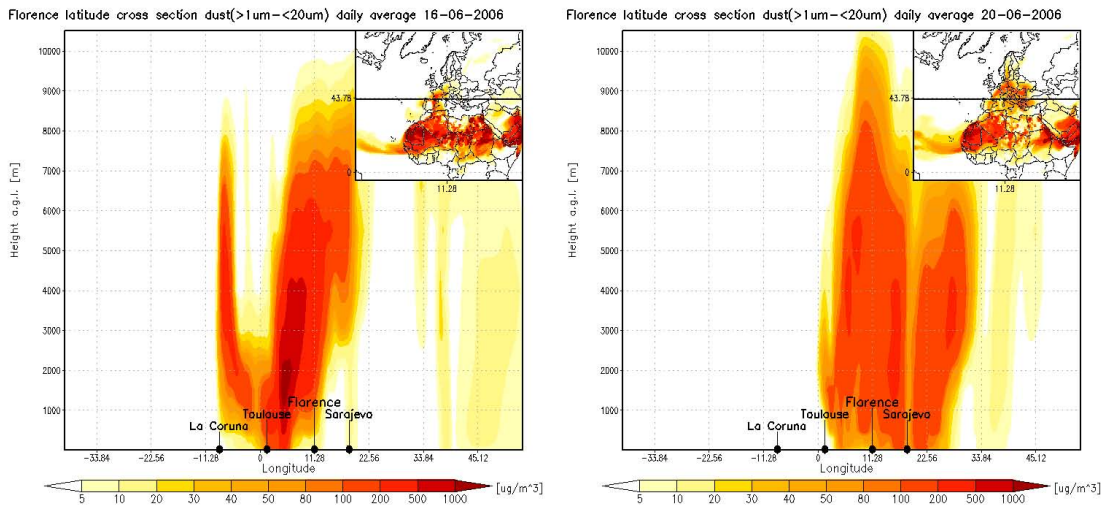


**Fig. 9.** Cross section at  $11.28^{\circ}$  E of the daily average of dust concentration, on 16 (left) and 20 June (right), particle size  $1\text{--}20\,\mu\text{m}$ .

[Title Page](#)[Abstract](#)[Introduction](#)[Conclusions](#)[References](#)[Tables](#)[Figures](#)[◀](#)[▶](#)[◀](#)[▶](#)[Back](#)[Close](#)[Full Screen / Esc](#)[Printer-friendly Version](#)[Interactive Discussion](#)

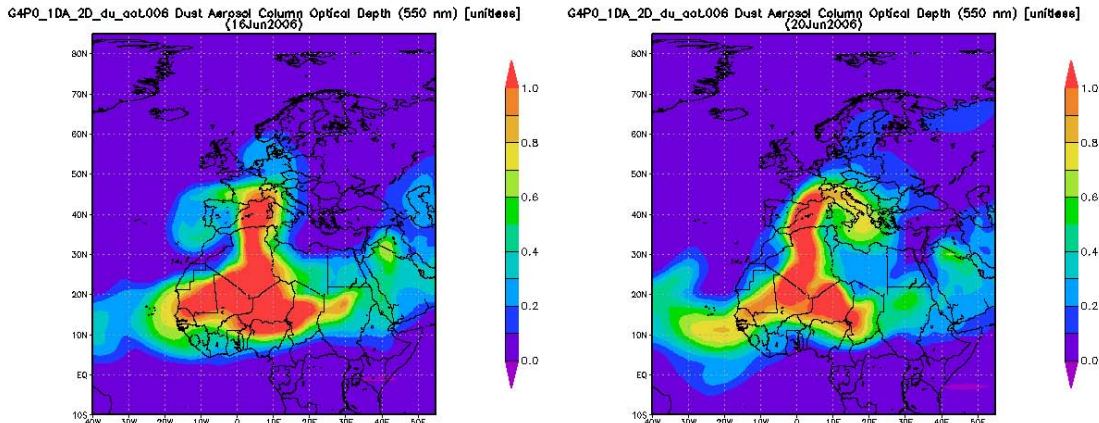


**Fig. 10.** Dust Aerosol Column Optical Depth (550 nm) from GOCART aerosol model data V006 ([http://disc.sci.gsfc.nasa.gov/gesNews/gocart\\_data\\_V006](http://disc.sci.gsfc.nasa.gov/gesNews/gocart_data_V006)), for 16 June 2006 (left) and 20 June 2006 (right).

Title Page

Abstract

Introduction

Conclusions

References

Tables

Figures

◀

▶

◀

▶

Back

Close

Full Screen / Esc

Printer-friendly Version

Interactive Discussion



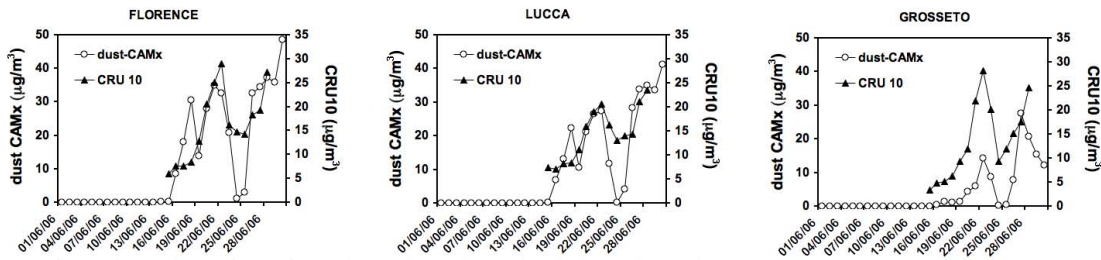


**Fig. 11.** Comparison between mean daily modelled concentrations (dust-CAMx) and crustal contribution to  $\text{PM}_{10}$  (CRU10), in Florence (left), in Lucca (center) and in Grosseto (right).

- [Title Page](#)
- [Abstract](#) [Introduction](#)
- [Conclusions](#) [References](#)
- [Tables](#) [Figures](#)
- [◀](#) [▶](#)
- [◀](#) [▶](#)
- [Back](#) [Close](#)
- [Full Screen / Esc](#)
- [Printer-friendly Version](#)
- [Interactive Discussion](#)